Electronic Supplementary Information

Spin reorientation and magnetic frustration in $Fe_{32+\delta}Ge_{35-x}Si_x$ with a kagome lattice broken by crystallographic intergrowth

*Roman A. Khalaniya, *,[a] Valeriy Yu. Verchenko,[a] Andrei V. Mironov,[a] Alexander N. Samarin,[b] Alexey V. Bogach,[a,b] Aleksandr N. Kulchu,[a] Alexey O. Polevik,[a] Zheng Wei,[c] Evgeny V. Dikarev,[c] Raivo Stern,[d] and Andrei V. Shevelkov[a]*

[a] Department of Chemistry, Lomonosov Moscow State University, 119991 Moscow, Russia

[b] Prokhorov General Physics Institute of the Russian Academy of Sciences, 119991 Moscow, Russia

[c] Department of Chemistry, University at Albany, Albany, 12222 New York, United States

[d] National Institute of Chemical Physics and Biophysics, 12618 Tallinn, Estonia

Table S1. The comparison between most important interatomic distances in $Fe_{32+\delta}Ge_{33}As_2$ [1], $Fe_{32+\delta}Ge_{35-x}P_x$ [2], and $Fe_{32+\delta}Ge_{35-x}Si_x$ at 100 K.

atom	atom	distance, Å		
		$Fe_{32.1}Ge_{33}As_2$	$Fe_{32.6}Ge_{33}Si_2$	$Fe_{32.6}Ge_{33}P_2$
As1/Ge0	As1/Ge0	2.503(2)	2.4754(14)	2.4658(9)
	Fe4 (×6)	2.5959(8)	2.5990(9)	2.5966(4)
	Fe5	2.5178(14)	2.5346(10)	2.5185(6)
Ge1	Ge1 (×2)	2.7205(8)	2.7119(10)	2.7514(5)
	Fe1 (×2)	2.4406(7)	2.4167(9)	2.4008(6)
	Fe3 (×2)	2.5074(9)	2.5005(8)	2.4622(4)
	Fe4 (×4)	2.4426(7)	2.4179(6)	2.3891(3)
	Fe5	2.7205(8)	2.7119(10)	2.7514(5)
Ge2	Ge2	2.8243(8)	2.8406(6)	2.8315(3)
	Fe1 (×2)	2.3026(6)	2.3080(8)	2.3073(5)
	Fe3 (×4)	2.5681(8)	2.5715(7)	2.5716(4)
Ge3	Ge5	2.9519(18)	2.9443(11)	2.9181(13)
	Fe1	2.3808(6)	2.3891(6)	2.3787(3)
	Fe2	2.3636(5)	2.3576(6)	2.3519(3)
	Fe3 (×2)	2.6095(4)	2.6059(8)	2.6019(3)
	Fe4 (×1)	2.5101(9)	2.5116(10)	2.5210(5)
Ge4	Ge5	2.721(3)	2.741(2)	2.7771(17)
	Ge5'	-*	-*	2.7198(4)
	Fe3 (×2)	2.4840(8)	2.4985(7)	2.4952(4)
	Fe4 (×4)	2.4216(7)	2.4291(6)	2.4340(4)
Ge5	Fe2		2.9033(15)	
	Fe3 (×4)	2.5669(9)	2.5723(11)	2.5680(5)
Ge5'	Fe3 (×4)	-*	-*	2.5060(3)
Fe1	Fe3 (×4)	2.8637(7)	2.8532(7)	2.8492(4)
	Fe4 (×1)	2.7287(10)	2.6900(8)	2.6637(4)
Fe3	Fe3	2.7216(10)	2.7236(10)	2.7397(5)
	Fe4 (×2)	2.7367(7)	2.7231(8)	2.7144(4)
Fe4	Fe4 (×2)	2.543(2)	2.5418(9)	2.5330(5)

** The Ge5' site is not occupied in $Fe_{32+\delta}Ge_{33}As_2$ and $Fe_{32+\delta}Ge_{35-x}Si_x$.*

Table S2. Summary of the results of the synchrotron HRPD experiments for the $Fe_{32+\delta}Ge_{35-x}Si_x$ powder samples.

initial composition	$Fe_{32.7}Ge_{31}Si_4$	$Fe_{32.7}Ge_{30}Si_5$	$Fe_{32.7}Ge_{29}Si_6$
refined composition	$Fe_{32.867(7)}$ $Ge_{31.39(2)}$ $Si_{3.61(2)}$	$Fe_{32.957(9)}$ $Ge_{30.45(3)}$ $Si_{4.55(3)}$	$Fe_{32.986(7)}$ $Ge_{29.96(2)}$ $Si_{5.04(2)}$
molar weight	4215.5	4178.7	4158.4
crystal system	hexagonal		
space group	*P*6/*mmm* (191)		
a, Å	11.87356(1)	11.85359(1)	11.84249(1)
c, Å	7.585117(6)	7.57948(1)	7.574371(8)
V, Å^3	926.093(1)	922.295(2)	919.948(2)
Z	1		
ρ_{calc}, g/cm^3	7.5562	7.5211	7.5036
radiation/wavelength	synchrotron/0.35451 Å		
temperature, K	293		
sample form	powder		
colour	metallic black		
2θ range, °	1.002–37.914	1.002–37.914	1.002–37.952
number of parameters	73	72	63
number of reflections	1215	1215	1215
GoF	1.39	1.97	1.53
$\Delta\rho_{max}/\Delta\rho_{min}$, e/Å^3	1.87/−2.12	2.70/−3.84	1.74/−2.64
$R_1[F^2 > 3\sigma(F^2)]^a$/w$R_2$, %	3.22/2.19	4.37/2.89	3.21/2.79

Table S3. Atomic parameters for the $Fe_{32.7}Ge_{31}Si_4$ powder sample at T = 293 K.

Atom	Wyck.	x	y	z	U_{eq}, Å^2	occupancy
Fe1	6*m*	0.21066(5)	2*x*	1/2	0.0051(4)	1
Fe2	2*c*	1/3	2/3	0	0.0079(6)	1
Fe3	12*n*	0.38418(7)	0	0.27953(10)	0.0080(3)	1
Fe4	12*o*	0.12288(4)	2*x*	0.23880(10)	0.0063(3)	1
Fe5	1*b*	0	0	1/2	0.0149(12)	0.867(7)
Ge0	2*e*	0	0	0.16180(19)	0.0071(4)	1
Ge1	6*k*	0.22848(11)	0	1/2	0.0055(5)	0.398(3)
Si1	6*k*	0.22848(11)	0	1/2	0.0055(5)	0.602(3)
Ge2	6*m*	0.43142(4)	1−*x*	1/2	0.0077(3)	1
Ge3	12*o*	0.24444(3)	2*x*	0.19705(8)	0.0131(2)	1
Ge4	6*j*	0.27075(7)	0	0	0.0080(3)	1
Ge5	6*l*	0.47626(9)	1−*x*	0	0.0211(10)	0.5

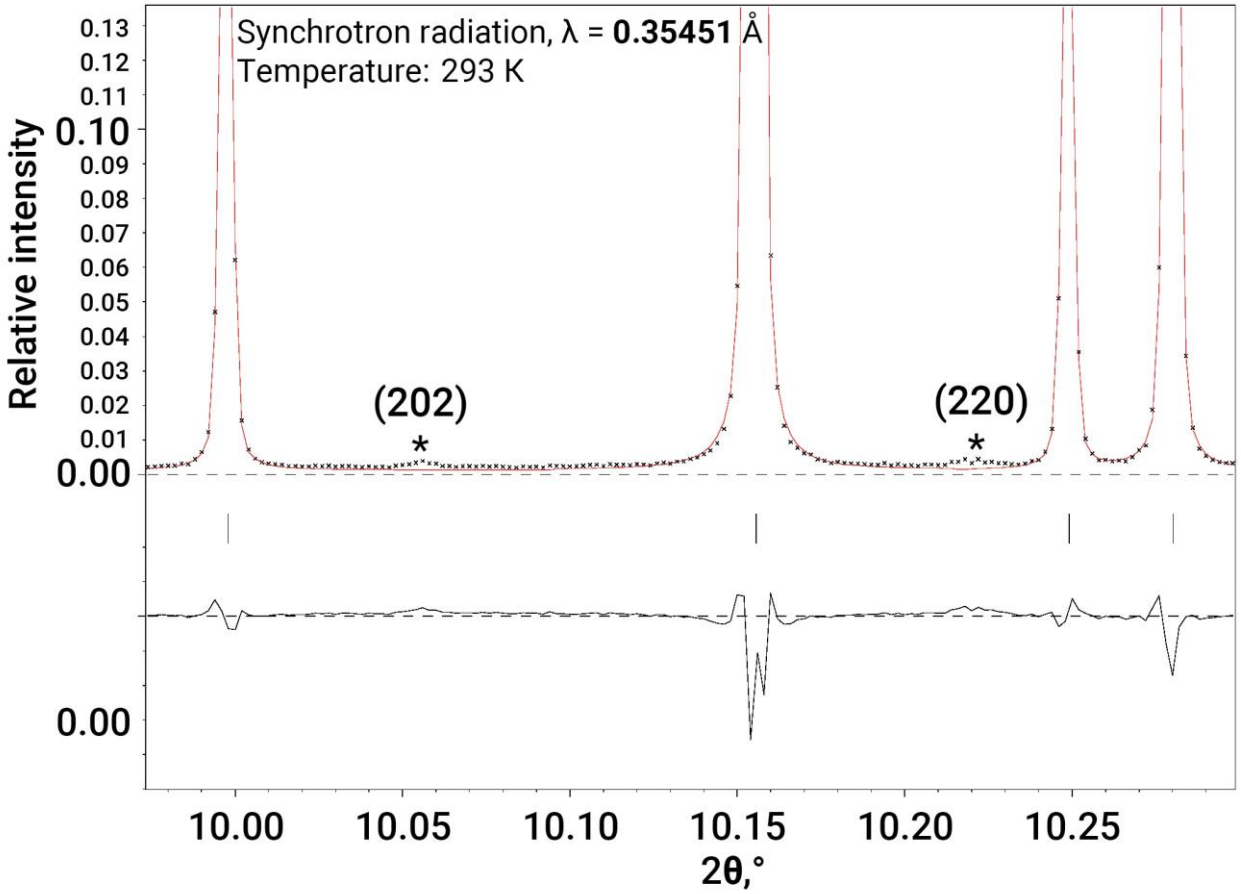

Fig. S1. A closeup of the region between 10.00 and 10.25 degrees of the high-resolution X-ray diffraction pattern of the $Fe_{32.7}Ge_{31}Si_4$ powder sample at room temperature. The positions of the main Bragg peaks of the η-$Fe_{7-\delta}Ge_4$ phase are marked by asterisks. For the full pattern, see the main text. The experimental diffraction pattern is shown as black dots, the red line represents the calculated pattern. Peak positions are given by the black ticks. The difference plot is shown by the black line in the bottom part.

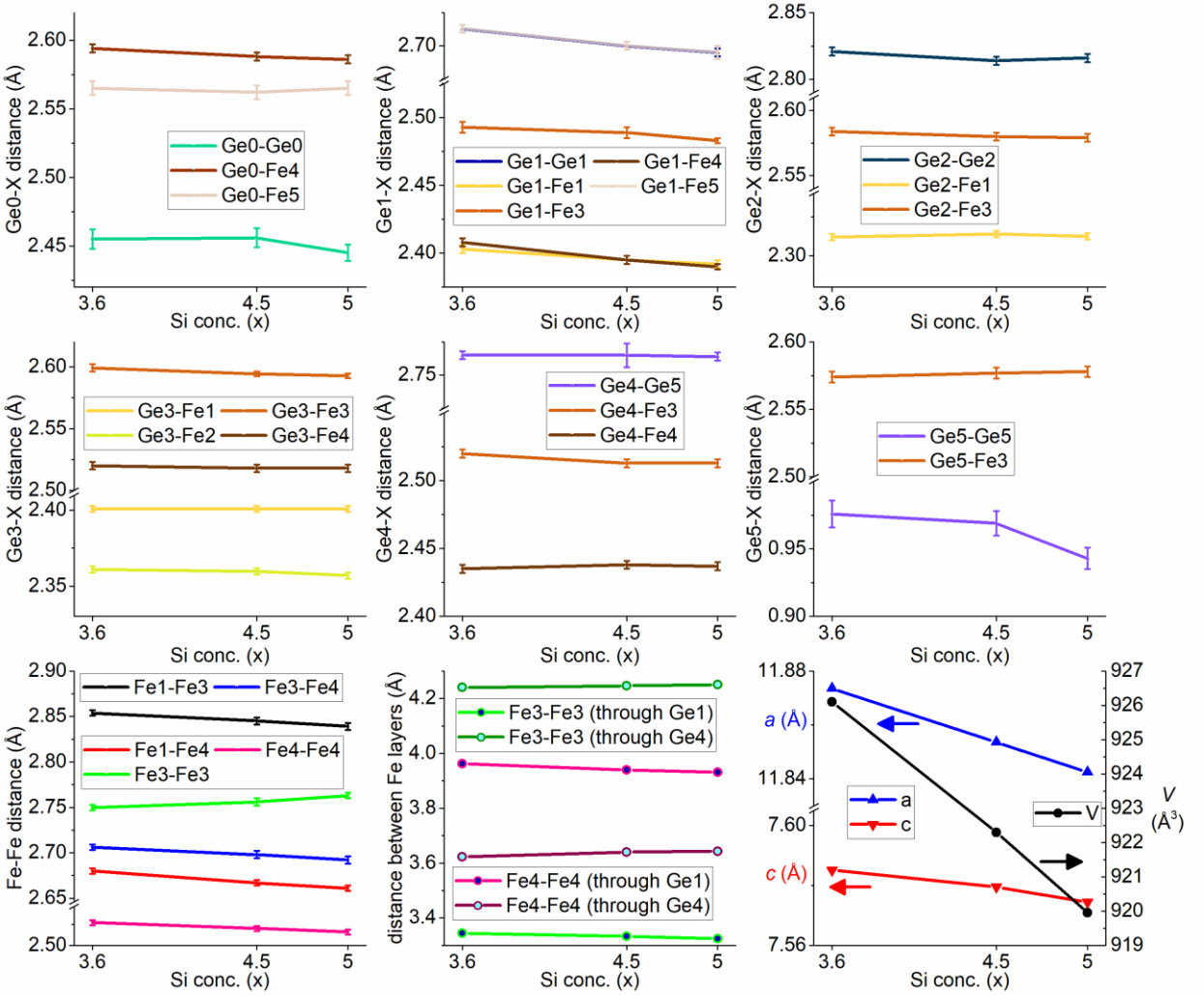

Fig. S2. Composition dependence of the interatomic distances in $Fe_{32+\delta}Ge_{35-x}Si_x$ based on the synchrotron HRPD data. The error bars are not shown on bottom-middle and bottom-right graphs, since they are too small to be properly displayed and are well within the symbols representing the datapoints.

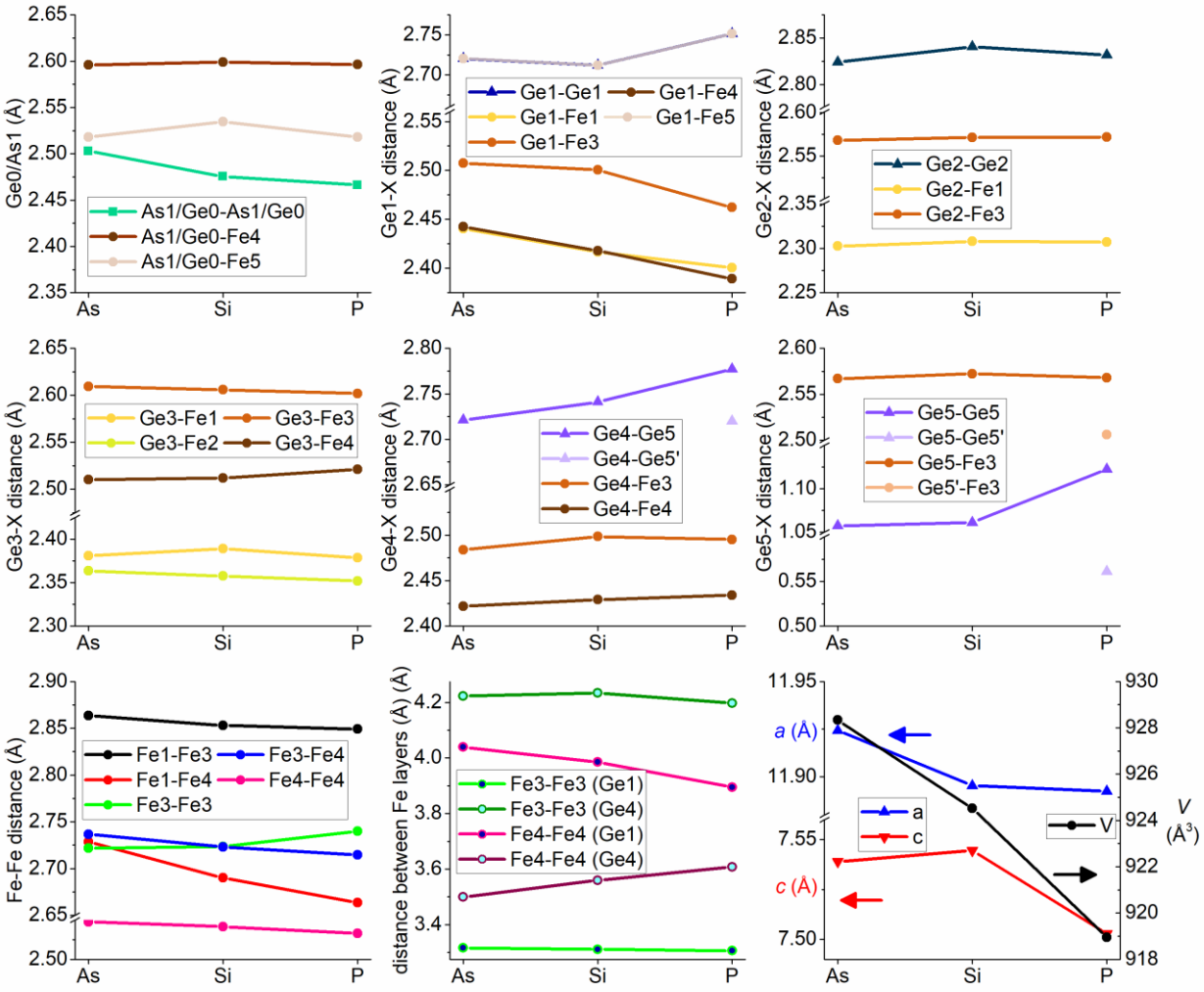

Fig. S3. Comparison between interatomic distances in $Fe_{32.1}Ge_{33}As_2$ [1], $Fe_{32.6}Ge_{33}Si_2$, and $Fe_{32.6}Ge_{33}P_2$ [2] at 100 K. The error bars are not shown since they are too small to be properly displayed and are well within the symbols representing the datapoints.

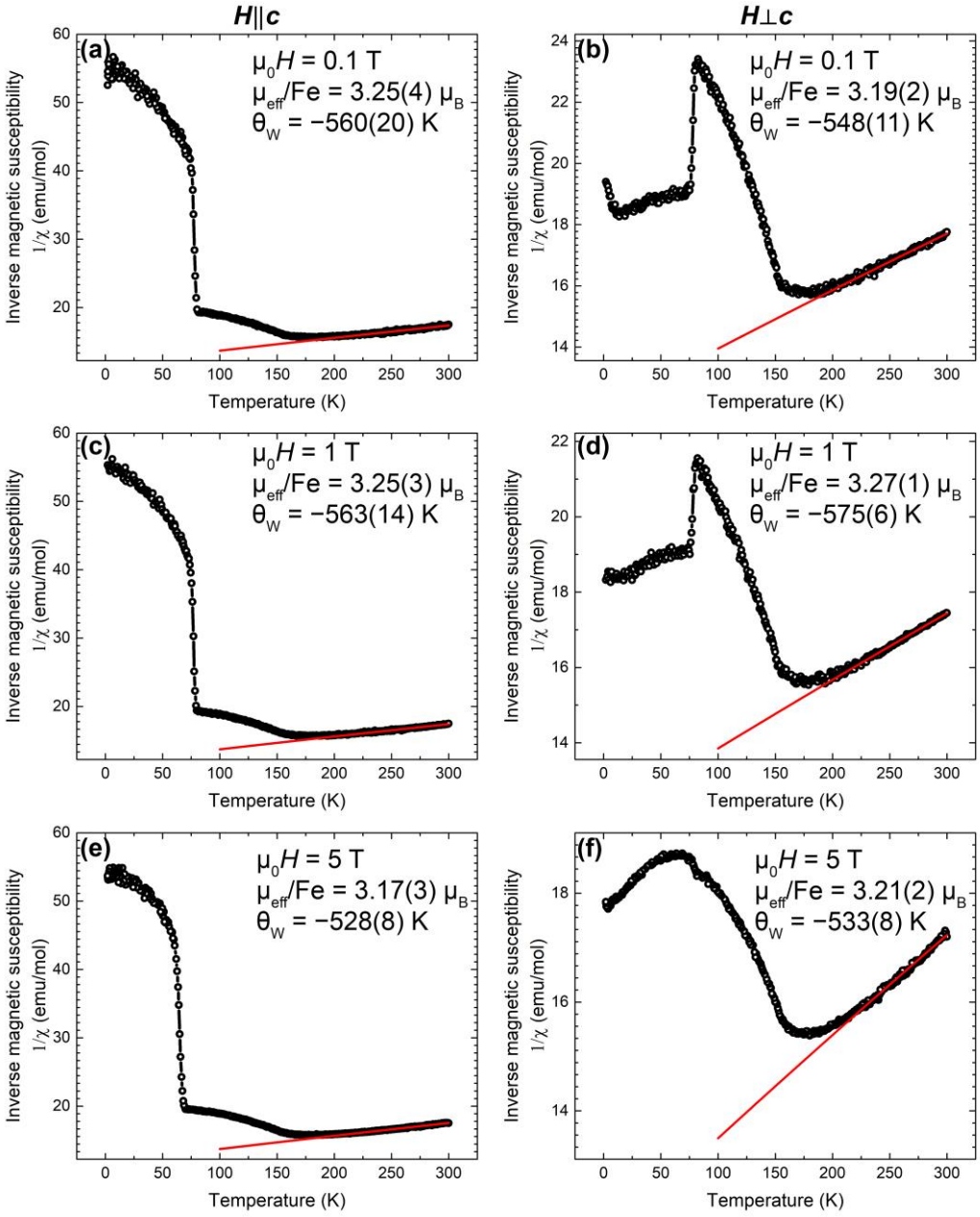

Fig. S4. Inverse magnetic susceptibility of the $Fe_{32.8}Ge_{30}Si_5$ single crystal in various magnetic fields. Black dots and lines represent the experimental data; the red lines show the Curie-Weiss fit performed in the range of 225−300 K. The refined Curie-Weiss parameters are shown in the respective graphs. The Curie-Weiss fit was performed using the modified Curie-Weiss law: $\chi = C/(T - \theta_W) + \chi_0$, where C is the Curie constant, θ_W is the Weiss temperature, χ_0 is the temperature independent contribution to the susceptibility. The latter was taken from the Curie-Weiss approximation of the $Fe_{32+\delta}Ge_{33}As_2$ magnetic susceptibility measured in a similar setup [1], since the Curie-Weiss fit of the high temperature susceptibility of $Fe_{32.8}Ge_{30}Si_5$ was unstable if χ_0 was refined. The effective moment per Fe atom μ_{eff}/Fe was calculated as $\mu_{eff}/Fe = \sqrt{\frac{3k_B C}{n_{Fe} N_A \mu_B}}$, where n_{Fe} is the number of Fe atoms in the formula unit, k_B is the Boltzmann constant, N_A is the Avogadro number, and μ_B is the Bohr magneton.

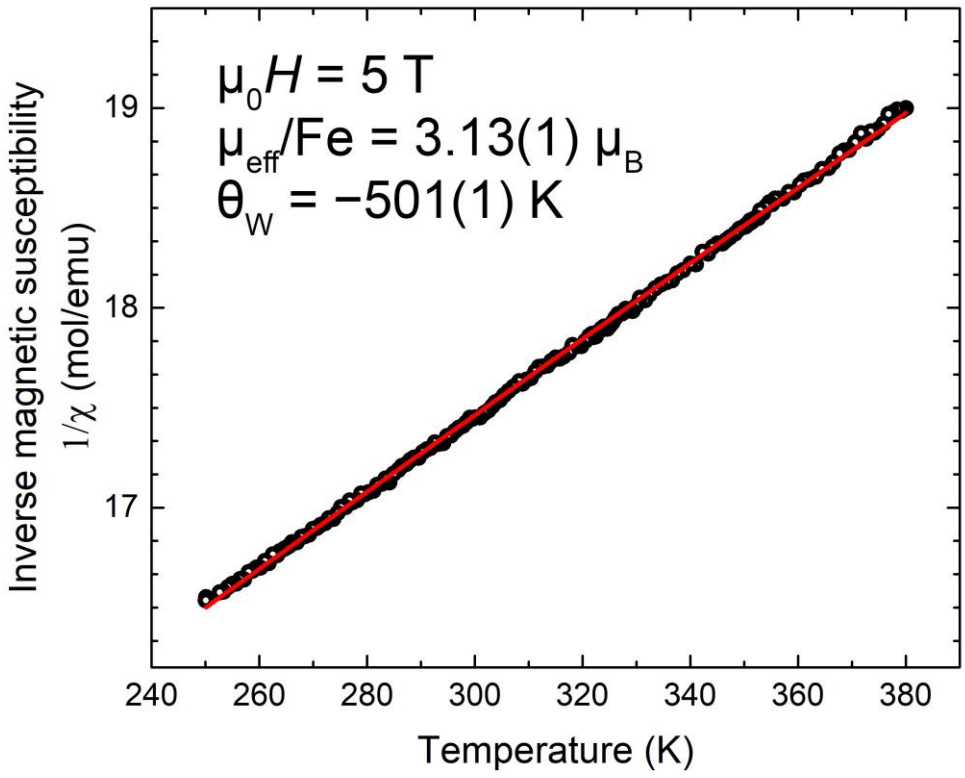

Fig. S5. Inverse magnetic susceptibility of the $Fe_{32.8}Ge_{30}Si_5$ twinned crystal in an applied field of 5T. Black dots and lines represent the experimental data; the red lines show the Curie-Weiss fit performed in the range of 250−380 K. The refined Curie-Weiss parameters are shown on the graph. For the details of the Curie-Weiss fit, see Figure S4.

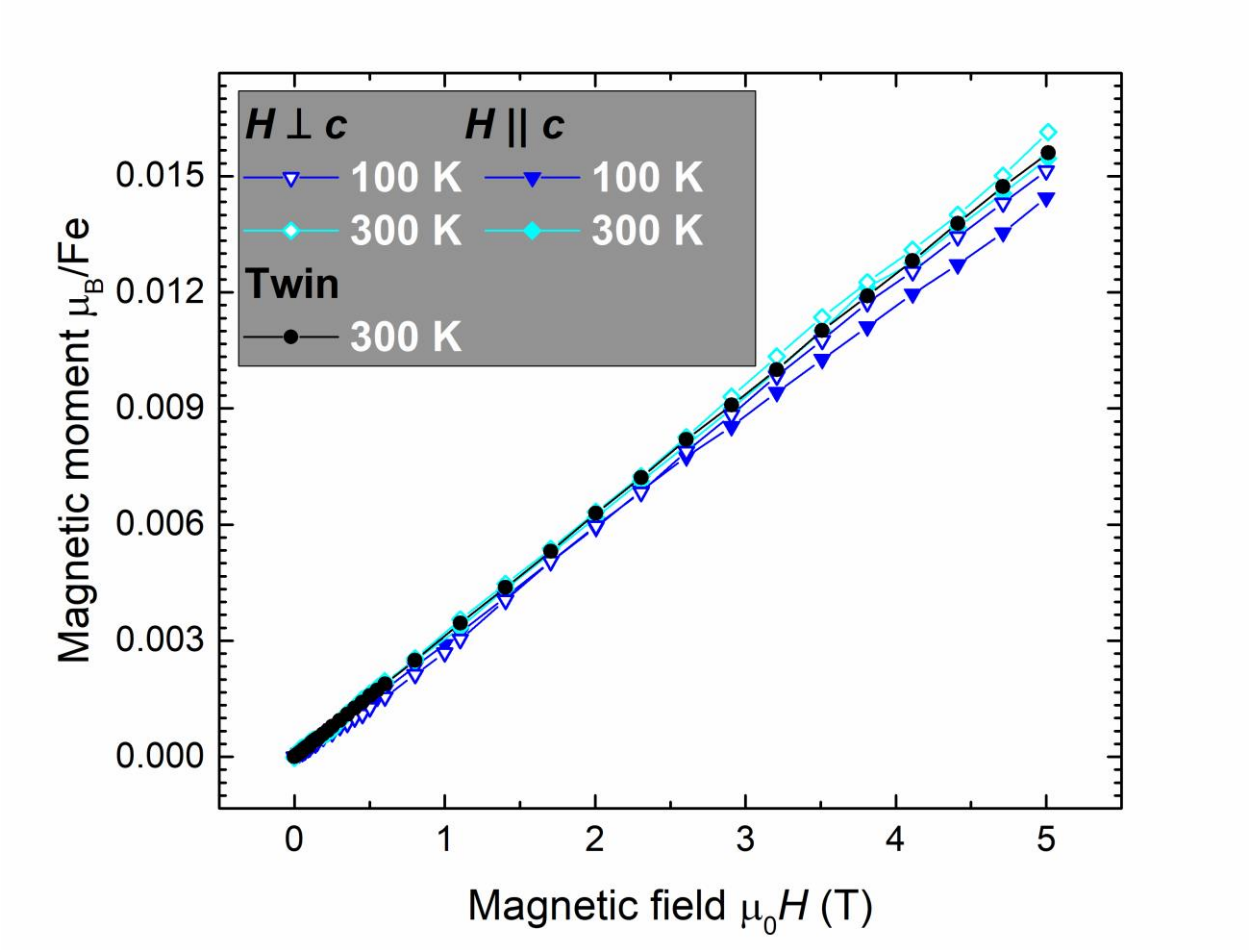

Fig. S6. Field dependence of the magnetisation of the $Fe_{32.8}Ge_{30}Si_5$ single crystal at 100 and 300 K and of the $Fe_{32.8}Ge_{30}Si_5$ twinned crystal at 300 K.

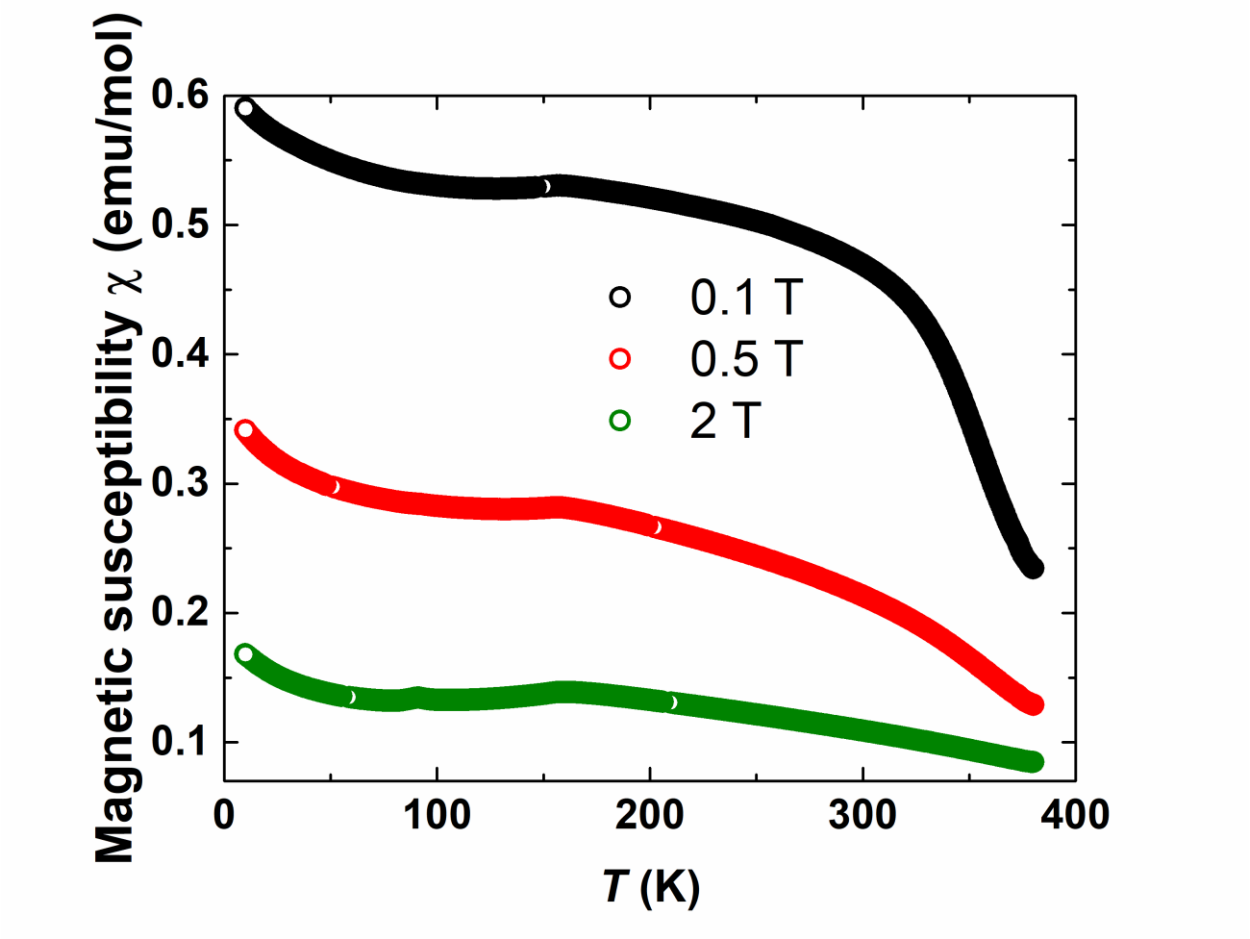

Fig. S7. Temperature dependence of the magnetic susceptibility of the $Fe_{32.7}Ge_{31}Si_4$ powder in applied fields $\mu_0 H$ = 0.1-2 T.

References

1. Khalaniya, R.A., Mironov, A.V., Verchenko, V.Y., Jesche, A., Tsirlin, A.A., Shevelkov, A.V. Nontrivial recurrent intergrowth structure and unusual magnetic behavior of intermetallic compound $Fe_{32+\delta}Ge_{33}As_2$. *Inorg. Chem.* (2016) *55*(24), 12953-12961.
2. Khalaniya, R.A., Verchenko, V.Y., Wei, Z., Dikarev, E.V., Heinmaa, I., Stern, R., Jesche, A., Tsirlin, A.A., Shevelkov, A.V., From $Fe_{32+\delta}Ge_{35-x}P_x$ to $Fe_{32+\delta}Ge_{35-x-y}P_xAs_y$: Fine geometry optimization in new intergrowth structures. *J. Alloys Compd.* (2019) *779*, 229-236.